J Arid Land
https://doi.org/10.1007/s40333-019-0012-y

Science Press Springer-Verlag

Actual evapotranspiration of subalpine meadows in the Qilian Mountains, Northwest China

GAO Yunfei[1], ZHAO Chuanyan[2*], Muhammad W ASHIQ[3], WANG Qingtao[1], RONG Zhanlei[1], LIU Junjie[1], MAO Yahua[2], GUO Zhaoxia[2], WANG Wenbin[1]

[1] State Key Laboratory of Grassland and Agro-Ecosystems, School of Life Sciences, Lanzhou University, Lanzhou 730000, China;
[2] State Key Laboratory of Grassland and Agro-Ecosystems, College of Pastoral Agriculture Science and Technology, Lanzhou University, Lanzhou 730000, China;
[3] Ministry of Natural Resources and Forestry, Timmins District, 5520 Hwy 101 E, South Porcupine, ON, P0N1H0, Canada

Abstract: As a main component in water balance, evapotranspiration (ET) is of great importance for water saving, especially in arid and semi-arid areas. In this study, the FAO (Food and Agriculture Organization) Penman-Monteith model was used to estimate the magnitude and temporal dynamics of reference evapotranspiration (ET_0) in 2014 in subalpine meadows of the Qilian Mountains, Northwest China. Meanwhile, actual ET (ET_c) was also investigated by the eddy covariance (EC) system. Results indicated that ET_c estimated by the EC System was 583 mm, lower than ET_0 (923 mm) estimated by the FAO Penman-Monteith model in 2014. Moreover, ET_0 began to increase in March and reached the peak value in August and then declined in September, however, ET_c began to increase from April and reached the peak value in July, and then declined in August. Total ET_c and ET_0 values during the growing season (from May to September) were 441 and 666 mm, respectively, which accounted for 75.73% of annual cumulative ET_c and 72.34% of annual cumulative ET_0, respectively. A crop coefficient (k_c) was also estimated for calculating the ET_c, and average value of k_c during the growing season was 0.81 (ranging from 0.45 to 1.16). Air temperature (T_a), wind speed (u), net radiation (R_n) and soil temperature (T_s) at the depth of 5 cm and aboveground biomass were critical factors for affecting k_c, furthermore, a daily empirical k_c equation including these main driving factors was developed. Our result demonstrated that the ET_c value estimated by the data of k_c and ET_0 was validated and consistent with the growing season data in 2015 and 2016.

Keywords: actual evapotranspiration; reference evapotranspiration; crop coefficient; meteorological factors; biotic factors

Citation: GAO Yunfei, ZHAO Chuanyan, Muhammad W ASHIQ, WANG Qingtao, RONG Zhanlei, LIU Junjie, MAO Yahua, GUO Zhaoxia, WANG Wenbin. 2019. Actual evapotranspiration of subalpine meadows in the Qilian Mountains, Northwest China. Journal of Arid Land, 11(3): 371–384. https://doi.org/10.1007/s40333-019-0012-y

1 Introduction

Water balance strongly influences the structure, function, and productivity of terrestrial ecosystems (Burman and Pochop, 1994). A critical component of water balance is actual evapotranspiration (ET_c) (Mitchell et al., 2009; Valipour et al., 2017), and determination of water balance depends on precise estimation of ET_c (Jensen et al., 1990; Allen et al., 1994; Jensen et al.,

*Corresponding author: ZHAO Chuanyan (E-mail: nanzhr@lzb.ac.cn)
Received 2017-10-31; revised 2018-07-28; accepted 2018-08-28

1997; Allen et al., 1998; ASCE-EWRI, 2005; Veroustraete et al., 2008; Allen et al., 2011; Semalty et al., 2011; Hssaine et al., 2018). Understanding of ET_c is also important for water utilization and management, especially in arid and semi-arid regions (Li et al., 2014; Zhao and Zhao, 2014). Qilian Mountains, located in Northwest China, are water sources for many inland rivers in Hexi Corridor. Subalpine meadows (grasslands) are a major land use in these mountains where heavy grazing not only impacts grass growth conditions but also affects ET. Therefore, it is imperative to estimate ET_c of these alpine meadows with consideration of grazing impact on ET_c.

A number of methods and models have been developed and used to estimate ET_c such as Bowen (Ohmura, 1982; Sun et al., 2006; Fang et al., 2018), Lysimeter (Howell et al., 1991; Gao et al., 2015), eddy covariance (EC) (Swinbank, 1951; Massman, 2000), water balance (Mastrorilli et al., 1998; Saadi et al., 2018) and FAO (Food and Agriculture Organization) Penman-Monteith (P-M) model (Allen et al., 1998). This study focused on two methods: EC and FAO Penman-Monteith model. The EC is a micro-meteorological approach widely used to study ET_c at the ecosystem level (Massman, 2000; Falge et al., 2001; Aubinet et al., 2012). The FAO Penman-Monteith model is a modified version of P-M model (Monteith, 1965) recommended by the FAO to estimate ET_c for various land uses including grassland (Allen et al., 1998). For each land use, ET_c is estimated using reference evapotranspiration (ET_0) values which in turn depend on land use specific crop coefficient (k_c) (Allen et al., 1998; Yang et al., 2013; Khoshravesh et al., 2017). The k_c values, for a specific land use, are generally assigned by the growth stage of the plants species. For example, the k_c values of 0.40, 1.05, and 0.85 in grasslands are respectively reported for initial-, middle-, and late-season growth stages of grass (Allen et al., 1998). Studies also show that some additional factors, such as meteorological data and vegetation biomass, also affect k_c value (Lockwood, 1999; Williams and Ayars, 2005; Zhou and Zhou, 2009; Yang and Zhou, 2011; Zhang et al., 2012). Therefore, accurately calculating k_c can provide more reliable estimation of ET_c.

The ET_c for subalpine meadows in the Qilian Mountains has been estimated (ranging from 2.88 to 3.26 mm/d) using micro-lysimeter method (Song et al., 2004; Yang et al., 2013). However, the ET_c estimation by micro-lysimeter is influenced by the weather conditions, i.e., it might be over-estimated during sunny days and under-estimated during rainy weather (Zhang et al., 2012; Zhou and Zhou, 2009). Thus, it is unsuitable for long-term ET_c estimation during all weather conditions. To fill this knowledge gap for grasslands in the Qilian Mountains, we used (1) EC system to observe ET_c at daily time scale, and (2) FAO Penman-Monteith model to estimate ET_0. The objectives of this study are (1) to estimate ET_c based on k_c and ET_0 values of the subalpine grasslands in the Qilian Mountains, and (2) to develop and validate a model of k_c based on meteorological factors and vegetation biomass of subalpine grasslands in the Qilian Mountains.

2 Materials and methods

2.1 Study area

The study area is located in Tianlaochi Catchment in the upper reaches of the Heihe River (38°23′56″–38°26′47″N, 99°53′57″–99°57′10″E) with the elevation ranging from 2660 to 4400 m a.s.l. (Fig. 1). Experimental site for this study is located at 3070 m altitude in subalpine meadow in the Qilian Mountains. The study area belongs to a typical alpine semi-arid climate, characterized by long and cold winters, and short and warm summers. The mean annual precipitation is about 435.0 (±5.6) mm with 84.2% precipitation occurring during May to September. The annual mean temperature is about −0.6°C–2.0°C, and mean January and mean July temperatures are –13.1°C and 12.1°C, respectively. The soil type is mountain grey cinnamon with up to 50 cm depth and gravel below 50 cm. Vegetation community mostly belongs to annual grasses, i.e., *Elymusnutans griseb* and *Foeniculum vulgare*, and their roots grow up to 30 cm.

2.2 Data collection

2.2.1 Meteorological and soil physical data

At the study site, a weather station and an EC system were set up in 2011 and 2013, respectively. Table 1 shows the list of meteorological factors for which data are being collected at half an hour intervals and soil physical data at the study site.

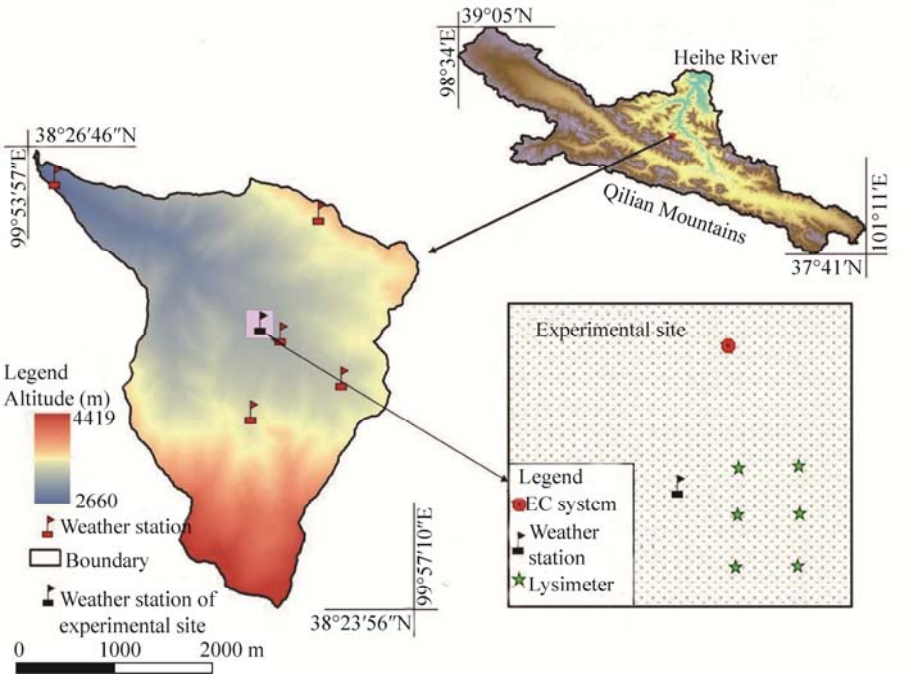

Fig. 1 Geographic location of the study area and distribution of observation instruments in the experimental site. EC, eddy covariance.

Table 1 Summary of the meteorological and soil physical data observed at the weather station

Parameter	Company	Country	Observational elevation	Abbreviation
Net radiation	Gene	USA	2 m	R_n
Short wave radiation	Gene	USA	2 m	R_s
Soil heat flux	Gene	USA	–5 cm	G
Wind speed	Hobo	USA	2 m	u
Air temperature	Hobo	USA	2 m	T_a
Relative humidity	Hobo	USA	2 m	RH
Pressure	Hobo	USA	2 m	P_a
Precipitation	Hobo	USA	1.8 m	P
Soil temperature	Decagon	USA	–5, –10, –20, and –50 cm	T_{s5}, T_{s10}, T_{s20}, and T_{s50}
Soil water content	Decagon	USA	–5, –10, –20, and –50 cm	SWC_5, SWC_{10}, SWC_{20}, and SWC_{50}

2.2.2 Flux measurements

The EC system was used to measure CO_2 fluxes, sensible heat (H), and latent heat (LE) at 2.2 m above the ground surface from 2013. A CO_2/H_2O infrared analyzer (Li-7550; LI-COR, Inc., Lincoln, NE, USA) and a three-dimensional supersonic anemometer (CSAT-3; Campbell Scientific, Inc., UT, USA) were mounted on a horizontal bar extending from a tower. The CO_2/H_2O sensor was installed in down-wind direction of supersonic anemometers. The CO_2/H_2O analyzer was calibrated after every six months. Short wave radiation (R_s) from the sky and long wave radiation (R_l) from the land surface were measured with a net radiometer (CNR-1; Kipp and Zonen, Delft, The Netherlands) at 1.5 m above the ground surface. The net radiation (R_n) was calculated from the difference of R_s and R_l. Soil heat fluxes (G) were recorded by a net radiometer at 10 cm soil depth. The R_n was partitioned into H, LE, and G.

The energy balance ratio (r) was calculated using the following equation (Gu et al., 1999):

$$r = (\sum(LE + H)) / (\sum R_n - G)). \quad (1)$$

The item LE+H measured by the EC system seemed to be underestimated since the average

value of r was about 0.75 for the entire observation period from 2014 to 2016, which fell in the median region of reported energy closures (0.55–0.99) (Wilson et al., 2002). The lack of energy balance closure had also been reported by Stannard et al., (1994) and Aubinet et al. (2012), and energy balance closure had become accepted as an important new test of EC (Anderson et al., 1984; Mahrt, 1998). We were not trying to specify a particular cause for the imbalance because several possibilities may be involved in the lack of energy closure (Wilson et al., 2002).

In long-term field measurements, gaps in data are a known issue. The gaps in data occur either due to non-recording (instrument malfunction/power failure) or rejection of certain data that do not meet quality control requirements. The quality of flux data collected for this study was assessed through a widely adopted flag system (Mauder and Foken, 2004), which lead to discard some data recorded at night time. The data gap filling was therefore, performed using a lookup table approach that considered both covariation of fluxes with meteorological variables and the temporal autocorrelation of the fluxes (Falge et al., 2001; Reichstein et al., 2005).

2.2.3 Biotic data

At the experimental site, six quadrats (0.5 m×0.5 m) were randomly selected to collect aboveground biomass. Biomass was measured every three days by cutting the plants at ground level and loading the plants into sampling bags during the growing season (May–October). Each sample was numbered and dried at 65°C until a constant weight was obtained.

2.3 Methods

2.3.1 FAO Penman-Monteith model

The FAO Penman-Monteith model (Allen et al., 1998) was used to calculate ET_0, which is expressed as follows:

$$ET_0=\frac{1}{\lambda}\left(\frac{\Delta}{\Delta+\gamma^*}\right)(R_n-G)+\frac{\gamma}{\gamma^*+\Delta}\left(\frac{900}{T+275}\right)uD, \tag{2}$$

$$ET_{cm}=k_c ET_0, \tag{3}$$

$$\gamma^*=\gamma(1+0.33u), \tag{4}$$

where λ is the water latent heat of vaporization (MJ/kg); Δ is the slope of the vapor pressure versus temperature curve (kPa/°C); R_n is the net radiation (MJ/(m^2·d)); G is the soil heat flux (MJ/(m^2·d)); γ is the psychrometric constant (kPa/°C); T is the daily mean temperature at 2 m above the ground surface (°C); u is the wind speed at 2 m above the ground surface (m/s); D is the vapor pressure deficit (kPa); ET_{cm} is the estimated actual evapotranspiration (mm/d) using the FAO-P-M model; and k_c is the crop coefficient.

2.3.2 EC model

EC model was used to calculate the ET_c:

$$ET_c=1000LE/\lambda\rho_w, \tag{5}$$

where LE is the latent heat flux (MJ/(m^2·d)); λ is the water latent heat of vaporization (MJ/kg); and ρ_w is the water density (kg/m^3).

2.3.3 Crop coefficient (k_c)

The daily k_c was obtained by dividing ET_c values with ET_0 values for the year 2014. The obtained k_c was used to develop two models: one with meteorological factors only, and the other using both meteorological factors and biotic factors. Both models were developed using the data of 2014, and validated using the data of 2015 and 2016.

2.3.4 Evaluation methods

In the study, the linear correlation coefficient (R^2), slope, Relative Root-Mean-Squared Error (RRMSE), Coefficient of Determination (CD) and Index of Agreement (IA) were used to examine the extent of the differences between the calculated and observed values of ET_c. The slope was the relative between the straight line and horizontal axis. The R^2 value was used to assess the correlation between the prediction results with actual situation (Gao et al., 2013). The RRMSE was a measure of relative magnitude of residuals; and the models with smaller RRMSE value are desirable (Gao et al., 2015). The IA was a measure to evaluate the correlation between the

observed and simulated values, and IA values closer to 1 are desirable (Li et al., 2014). The CD was used to measure dispersion of simulated values from the mean observed values, and CD greater than 0.8 indicates that the result was acceptable (Cai et al., 2007). The R^2 and slope were calculated in Sigmaplot 11.0 (Alexandris and Kerkides, 2003; Yang and Zhou, 2011). The mathematical expressions of RRMSE, CD, and IA were presented as follows:

$$\mathrm{RRMSE}=\sqrt{\frac{\sum_{i=1}^{n}\left(O_i-E_i\right)^2}{n}}\times\frac{1}{\overline{O}^2}, \tag{6}$$

$$\mathrm{CD}=\frac{\sum_{i=1}^{n}\left(O_i-\overline{O}\right)^2}{\sum_{i=1}^{n}\left(E_i-\overline{O}\right)^2}, \tag{7}$$

$$\mathrm{IA}=1-\frac{\sum_{i=1}^{n}\left(E_i-O_i\right)^2}{\sum_{i=1}^{n}\left(\left|E_i-\overline{O}\right|+\left|O_i-\overline{O}\right|\right)^2}, \tag{8}$$

where O_i is the observed value; $\overline{O}$ is the mean observed value; E_i is the simulated value; and n is the number of samples.

2.3.5 Vapor pressure deficit (VPD)

VPD is the difference between the pressure of water vapor held in saturated air at a given temperature and the pressure of water vapor that exists in the ambient air. It is calculated as follows:

$$\mathrm{VPD}=0.61008\times e^{\frac{17.27\times T}{T+237.3}}\times\left(1-\frac{\mathrm{RH}}{100}\right), \tag{9}$$

where T is the daily mean temperature at 2 m above the ground surface (°C); RH is the relative humidity.

3 Results

3.1 Variations of meteorological and soil physical factors

Temporal variations in meteorological factors are shown in Figures 2 and 3. The mean daily values of R_n, R_s, T_a, VPD, and u were 12.43 MJ/(m^2·d), 22.40 MJ/(m^2·d), –0.57°C, 0.658 kPa and 1.21 m/s, respectively. During the growing season, the sequence of SWC was SWC_{20}>SWC_5>SWC_{10}>SWC_{50} and that of T_s (soil temperature) was T_{s5}>T_{s10}>T_{s20}>T_{s50}. Both T_a and R_n reached the minimum in December and the maximum in July. VPD reached the maximum of about 1.180 kPa during the growing season, whereas u reached the maximum in February and the minimum in July.

3.2 Monthly variations of ET_0 and ET_c

Figure 4a shows that annual ET_0 was 923 mm, which was higher than the annual ET_c (583 mm) in 2014. ET_0 gradually increased from January and reached the peak value in August and then declined in September. Whereas, ET_c began to greatly increase in April and reached the peak level in July and then it started to decline in August. The total ET_c and ET_0 values during the growing season (from May to September) were 441 and 666 mm, respectively, which accounted for 75.73% and 72.34% of annual ET_c and ET_0, respectively.

Figure 4b compares the temporal variation of ET_c and precipitation (P). The annual values of ET_c and P were 583 and 546 mm, respectively. The annual ratio of ET_c to P is 1.067. However, the values of ET_c and P during the growing season (from May to September) were 441 and 540 mm, respectively, and the ratio was 0.818.

3.3 Temporal variations of k_c

As shown in Figure 5, k_c quickly increased from May to June, and remained a high level in July and August. It declined in September and was about 0.2 at the end of October. During the growing season, k_c exhibited a mean value of 0.81 and fluctuated within the ranges of 0.45–1.16.

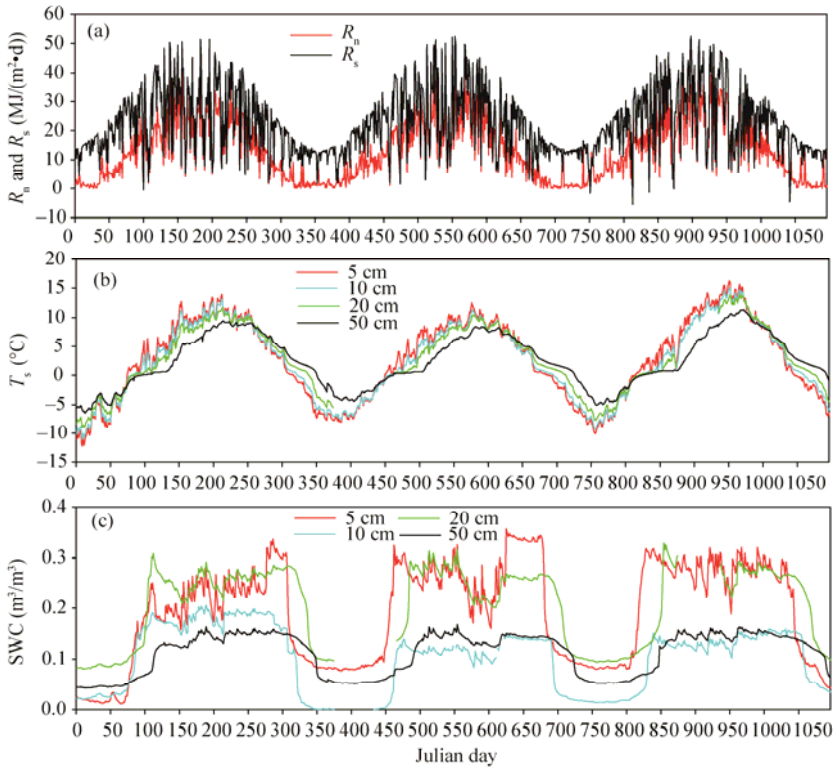

Fig. 2 Temporal variations of meteorological and soil physical factors from 2014 to 2016. (a) net radiation (R_n) and short wave radiation (R_s); (b) soil temperature (T_s) at the depths of 5, 10, 20, and 50 cm (i.e., T_{s5}, T_{s10}, T_{s20} and T_{s50}, respectively); (c) soil water content (SWC) at the depths of 5, 10, 20, and 50 cm (i.e., SWC_5, SWC_{10}, SWC_{20} and SWC_{50}, respectively).

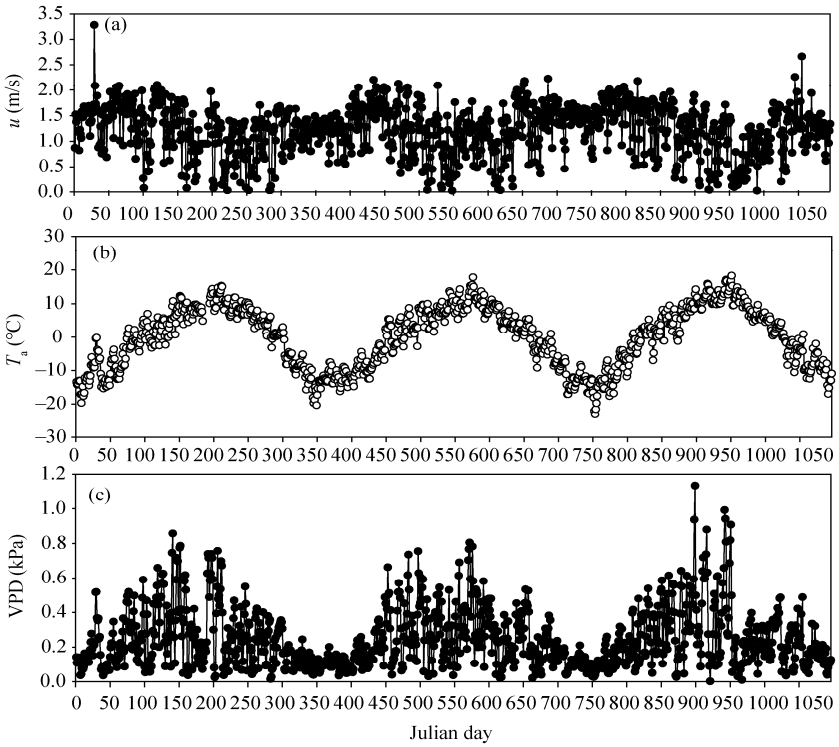

Fig. 3 Temporal variations of meteorological factors from 2014 to 2016. (a) mean wind speed (u) at the 2-m height; (b) air temperature (T_a); (c) vapor pressure deficit (VPD).

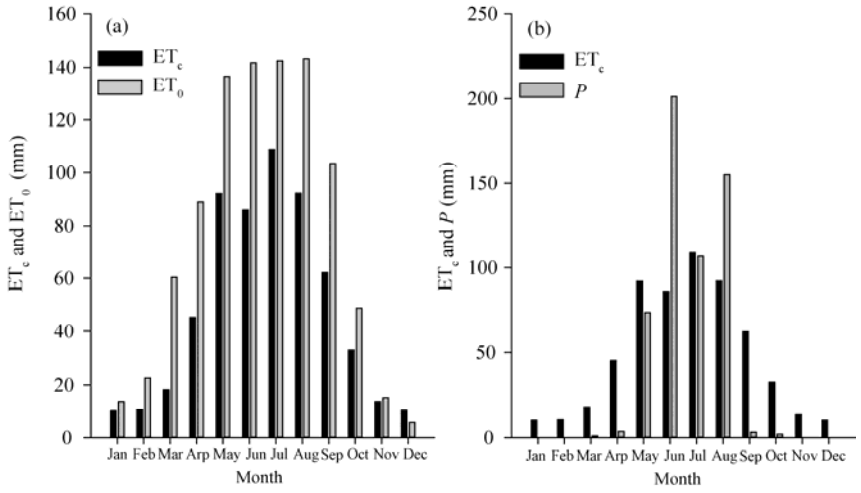

Fig. 4 Annual variations in actual evapotranspiration (ET_c) and reference evapotranspiration (ET_0). (a) annual variations in actual evapotranspiration and (b) precipitation (P).

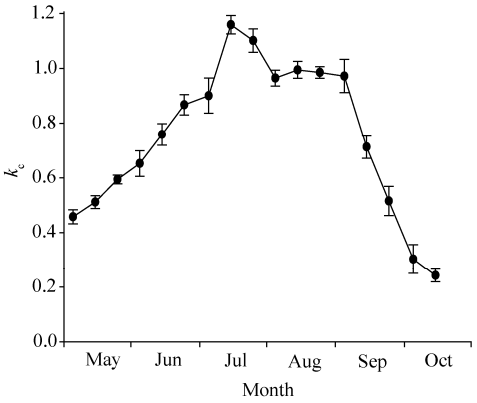

Fig. 5 Variation of crop coefficient (k_c) at 10-d intervals in 2014. Bars indicate standard errors.

3.4 Factors impacting k_c

3.4.1 Effect of environmental factors on k_c

In the study, the Pearson's product-moment correlation coefficients between k_c and environmental factors were computed at a daily scale (Table 2). The significant correlations (P<0.01) of k_c with u, T_a, R_n and T_{s5} suggest that these factors are critical for controlling k_c. The relationships of k_c with P, SWC_5, T_{s10} and T_{s20} were also significant (P<0.05).

The significant negative correlation between u and RH (Table 2) suggests the role of wind in the blowing away water vapours. The SWCs mainly come from precipitation, i.e., the infiltration into soil layer through rainfall, so there are good correlations between precipitation and SWC. Solar radiation provides energy to soil that in turn increases soil temperature. Using significant climatic factors (Table 2), we developed the following regression model to estimate daily k_c:

$$k_c = 0.650 + 0.224u - 0.038T_a - 0.030R_n - 0.002P + 0.570\mathrm{SWC}_5 + 0.110T_{s5} - 0.016T_{s10} - 0.009T_{s20}. \quad (10)$$

According to Equations 3 and 9, we calculated the daily ET_{cmod1} as follows:

$$\mathrm{ET}_{cmod1} = k_c \times \mathrm{ET}_0 = (0.650 + 0.224u - 0.038T_a - 0.030R_n - 0.002P + 0.570\mathrm{SWC}_5 + 0.110T_{s5} - 0.016T_{s10} - 0.009T_{s20}) \times \mathrm{ET}_0, \quad (11)$$

where ET_{cmod1} is the ET_c calculated by Equation 11.

Table 2 Pearson's product-moment correlation coefficients between daily crop coefficient (k_c) and meteorological and soil physical factors, i.e., wind speed (u), air temperature (T_a), relative humidity (RH), net radiation (R_n), air pressure (P_a), precipitation (P), soil water content (SWC) at the depths of 5, 10, 20 and 50 cm, and soil temperature (T_s) at the depths of 5, 10, 20 and 50 cm during the growing season in 2014

	k_c	u	T_a	RH	R_n	P_a	P	SWC_5	SWC_{10}	SWC_{20}	SWC_{50}	T_{s5}	T_{s10}	T_{s20}	T_{s50}
k_c	1.000														
u	0.194**	1.000													
T_a	0.177**	0.099	1.000												
RH	–0.109	–0.899**	–0.019	1.000											
R_n	–0.512**	0.037	0.203**	–0.012	1.000										
P_a	–0.139*	0.043	–0.090	–0.165*	–0.039	1.000									
P	–0.055	–0.356**	0.108	0.394**	0.169**	–0.169**	1.000								
SWC_5	–0.049*	–0.542**	–0.045	0.600**	–0.120*	–0.141**	0.155**	1.000							
SWC_{10}	0.028	–0.307**	0.077	0.383**	–0.004	–0.257**	–0.044	0.751**	1.000						
SWC_{20}	0.084	–0.079	0.072	0.151*	–0.005	–0.153**	–0.047	0.565**	0.741**	1.000					
SWC_{50}	0.122	–0.185*	0.470**	0.292**	0.107	–0.166**	0.106	0.582**	0.662**	0.666**	1.000				
T_{s5}	0.173**	–0.069	0.933**	0.189**	0.259**	–0.197**	0.237**	0.082	0.164**	0.148**	0.595**	1.000			
T_{s10}	0.150*	–0.184**	0.891**	0.306**	0.237**	–0.201**	0.280**	0.192**	0.241**	0.218**	0.679**	0.980**	1.000		
T_{s20}	0.119*	–0.320**	0.794**	0.442**	0.180**	–0.171**	0.265**	0.365**	0.375**	0.296**	0.778**	0.901**	0.962**	1.000	
T_{s50}	0.091	–0.403**	0.651*	0.514**	0.067	–0.119**	0.141**	0.530**	0.514**	0.342**	0.792**	0.744**	0.831**	0.942**	1.000

Note: ** and * indicate significance at 0.99 and 0.95 confidence levels, respectively.

3.4.2 Effects of biotic factors on k_c

Biomass directly reflects the conditions of a biological community, so we selected it as a biotic factor. The results showed that the biomass gradually increased in May, rapidly increased in June and July, and reached a peak in August (with a maximum of 505 g/m^2), and then began to decrease rapidly in September (Fig. 6).

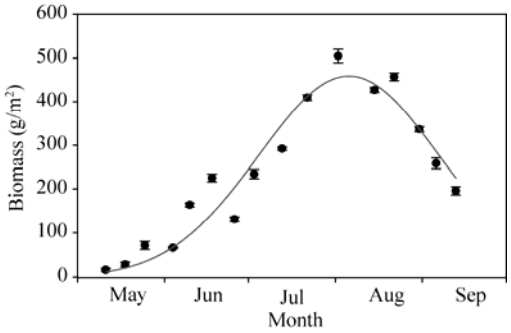

Fig. 6 Variation of biomass during the growing season in 2014. Bars indicate standard errors.

The regression analysis showed a significant positive correlation between biomass and k_c (Fig. 7). The linear regression equation is as follows:

$$k_c=0.0011\times\text{biomass}+0.5687. \quad (12)$$

Considering both meteorological and biotic factors, we calculated daily ET_{cmod2} as follows:

$$ET_{cmod2}=(0.650+0.224u-0.038T_a-0.030R_n-0.002P+0.570SWC_5+0.110T_{s5}-0.016T_{s10}-0.009T_{s20})\times(0.0011\times\text{biomass}+0.5687)\times ET_0, \quad (13)$$

where ET_{cmod2} is the ET_c calculated by Equation 13.

3.5 Testing estimated EC_c

We validated Equations 11 (ET_{cmod1}) and 13 (ET_{cmod2}) using the EC system data collected during the growing seasons in 2015 and 2016. The estimated values were close to the observed values (Fig. 8). The slope, R^2 and IA of ET_{cmod2} were greater than those of ET_{cmod1} (Table 3), implying that the correlation between observed values and simulated values by ET_{cmod2} is better than that by

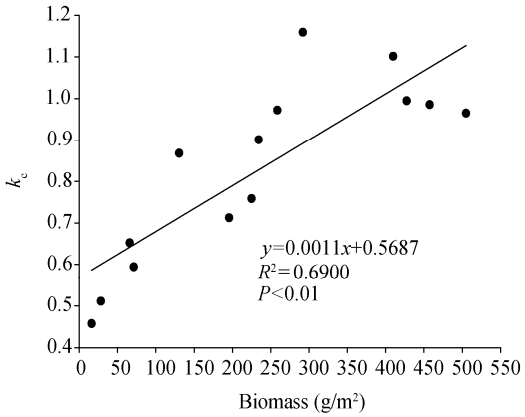

Fig. 7 Scatter plot between crop coefficient (k_c) and biomass

ET_{cmod1}. The RRMSE obtained by ET_{cmod2} was smaller than that by ET_{cmod1}, suggesting a higher accuracy of ET_{cmod2} than that of ET_{cmod1}. The values of CD for both ET_{cmod1} and ET_{cmod2} were greater than 0.8, indicating both regression equations are good. Overall, the performance of ET_{cmod2} that used both meteorological and biotic factors is better than that of ET_{cmod1} (only meteorological factors).

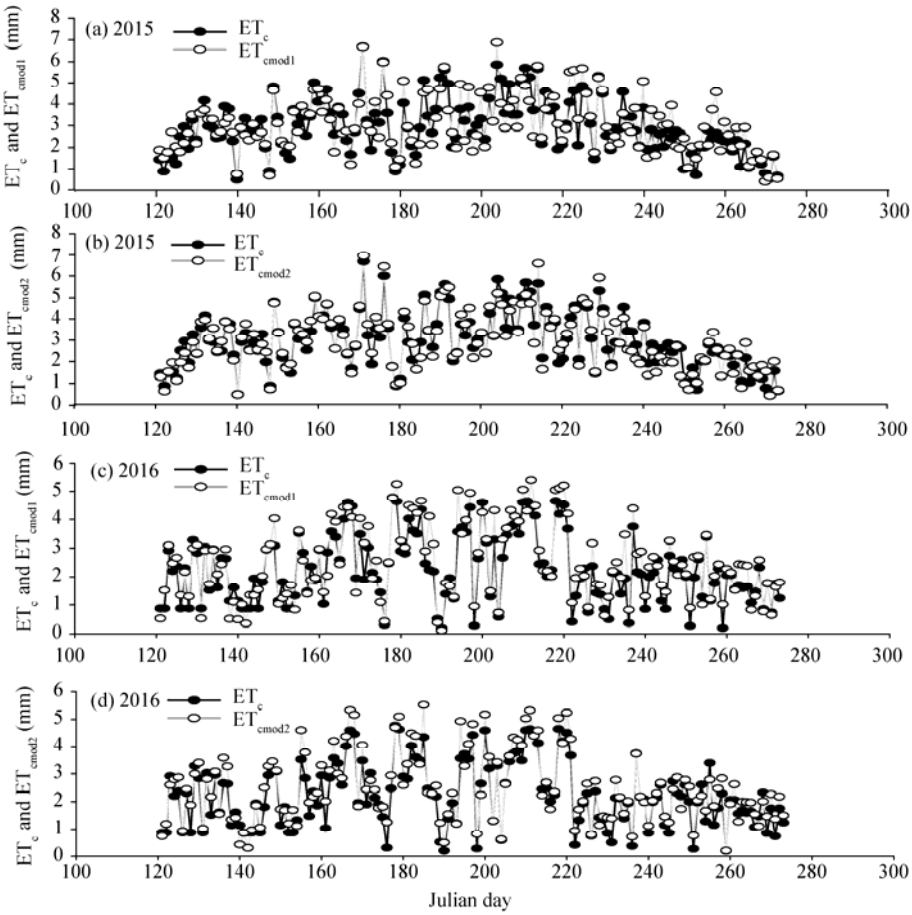

Fig. 8 Temporal variations of measured ET (ET_c) and simulated ET (ET_{cmod1}). (a) ET_c and ET_{cmod1} in 2015; (b) ET_c and ET_{cmod2} in 2015; (c) ET_c and ET_{cmod1} in 2016; and (d) ET_c and ET_{cmod2} in 2016.

Table 3 Summary of the parameters to assessing the accuracy of the two models

Variable	Slope		R^2		RRMSE		IA		CD	
	2015	2016	2015	2016	2015	2016	2015	2016	2015	2016
ET_{cmod1}	0.875	0.835	0.709	0.867	0.077	0.102	0.930	0.874	1.002	0.812
ET_{cmod2}	0.921	0.890	0.866	0.906	0.050	0.092	0.972	0.916	0.942	0.835

Note: R^2, correlation coefficient; RRMSE, Relative Root-Mean-Squared Error; IA, Index of Agreement; CD, Coefficient of Determination.

4 Discussion

4.1 Variations of ET_0, ET_c and P

The result shows that ET_c was lower than ET_0. The maximum of ET_0 appeared in August, and the minimum was in December. However, the maximum of ET_c appeared in July and the minimum occurred in December.

According to Equation 2, the meteorological and soil factors were the only factors that affected ET_0. However, the ET_c was affected not only by meteorological factors but also by biotic factors such as biomass, when R_s, R_n, T_a, and RH increased from April and reached the peak values in August and then declined (Figs. 2 and 3). ET_c began to increase in April and reached the maximum in July with the canopy development during the growing season.

The annual ratio of ET_c to P (i.e., 1.067) indicates that P was less than ET_c (Hou et al., 2011). However, the ratio of ET_c to P during the growing season (from May to September) was 0.818. This suggests that adequate water availability supports the plant growth in this period. The value of ET_0 during the growing season was 666 mm, and the ratio of ET_0 to P during the growing season was 1.240. This result was similar to the researches in some grassland ecosystems (Wever et al., 2002; Li et al., 2005). However, our result was higher than a non-irrigated pasture (Sumner and Jacobs, 2005) and an alpine winter pasture (Li et al., 2014).

ET process is governed by energy exchange at the vegetation surface and is limited by the amount of energy available (Semalty et al., 2011). ET_0 in our study area is caused by the climatic conditions. R_n in the study area was higher than that in the Qinghai-Tibetan Plateau grassland (Gu et al., 2008), so ET_0 was higher than that reported by Li et al. (2014) who conducted their study in the Qinghai-Tibetan Plateau grassland. Apart from energy enhancing the ET_0 in some extent, the high SWC and P could offer water for the need of plants (Yang and Zhou, 2011; Simona and Rita, 2013; Li et al., 2014). High T_s may inspire plant activity and make plant absorb more water (Gao et al., 2015), while low RH may improve the water vapor exchange between the atmosphere and vegetation (Gao et al., 2015).

4.2 Temporal variations of k_c

k_c quickly increased from May to June, remained at a high level in July and August, and then declined in September. The range of k_c in the study (0.45–1.16) was larger than that of k_c reported in FAO 56 (0.30–1.05) (Allen et al., 1998), and it was higher than that of k_c observed in an alpine winter pasture (0.30–0.92) (Li et al., 2014), in a typical steppe (0.32–0.68) (Miao et al., 2009) and in a temperate desert steppe of Inner Mongolia (0.02–0.50) (Yang and Zhou, 2011; Zhang et al., 2012). Our result indirectly showed that the subalpine meadows in the Qilian Mountains featured more adequate moisture and better plant growth conditions than the other semi-arid and arid grassland ecosystems.

4.3 Factors impacting k_c

The highest correlation between k_c and environmental factors suggested that R_n was the most important factor for determining k_c. Similar findings have been reported for an alpine winter pasture (Li et al., 2014). The higher R_n made a significant contribution to the k_c (Gao et al., 2015). However, Yang and Zhou (2011) selected a temperate desert steppe as their study area, which water was a key environmental factor pointed out that SWC was the most important factor, and Hou (2010) stated temperature was the most important meteorological factor. These differences may result from the different environmental conditions of plant growth.

In addition to meteorological factors, biotic factors can greatly affect k_c (Tyagi et al., 2000; Williams et al., 2003; De Medeiros et al., 2005; Li et al., 2014). Biomass directly reflects the conditions of a biological community, so we selected it as a biotic factor to estimate k_c.

Figure 9 shows that the EC calculated by both Equations 11 and 13 is underestimated in 2015 and 2016. FAO Penman-Monteith model performs well under the abundant water condition. The underestimation of ET_0 and ET_c, in our study area is likely due to the erratic precipitation which is not sufficient to meet water requirement criteria of FAO Penman-Monteith model.

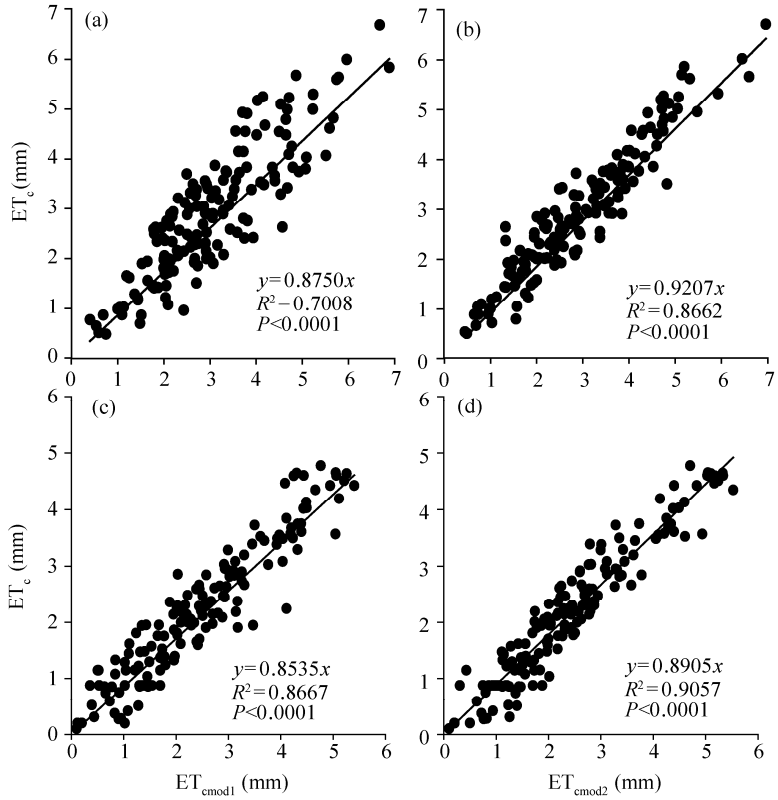

Fig. 9 Scatter plots between ET_c and ET_{cmod1} in 2015 (a), ET_c and ET_{cmod2} in 2015 (b), ET_c and ET_{cmod1} in 2016 (c), and ET_c and ET_{cmod2} in 2016 (d)

4.4 Testing estimated EC_c

Equations 11 (ET_{cmod1}) and 13 (ET_{cmod2}) were validated using the EC system data collected during the growing season in 2015. The simulated accuracy by the Equations 11 and 13 was compared using slope, R^2, RRMSE, IA, and CD.

The values of RRMSE were smaller, and the results of the model correlation were better. In Table 3, the slope, R^2 and IA of ET_{cmod1} were greater and the RRMSE was smaller than those of ET_{cmod2}, and the CD values of ET_{cmod1} and ET_{cmod2} were greater than 0.8. The results indicate that the fitting method that comprehensively considers meteorological factors and vegetation conditions can be used to derive simulated ET_c results that were closer to the actual observed ET_c results.

5 Conclusions

The FAO Penman-Monteith model was used to simulate the ET_0 over the subalpine meadows in the upper reaches of the Heihe River. Meanwhile, the ETc was measured by EC system. During the growing season, the ratio of ET_c to ET_0 is 0.663, and the ratio of ET_c to P is 0.818. Both ratios explained the habit of meadows in the study area is good. The k_c was used to estimate the ET_c. The average value of k_c during the growing season was 0.81 (ranging from 0.45 to 1.16). R_n, T_a, u,

and T_{s5} were the critical factors for controlling k_c. P_a, SWC_5, T_{s10} and T_{s20} also showed a significant relation to k_c. Finally, we developed a daily empirical k_c equation based on biomass, T_a, u, R_n, P, SWC_5, T_{s5}, T_{s10}, and T_{s20} to estimate the daily k_c, and used the k_c and ET_0 to estimate the ET_c. The model validation with 2015 and 2016 growing season data shows that the daily empirical k_c equation performed well in this study area.

Acknowledgements

This research was supported by the National Natural Science Foundation of China (41571051, 91425301). The authors would like to thank Dr. PENG Shouzhang and Dr. YUAN Liming for their help with setting up the EC system and weather station. Thanks to Gansu Qilianshan National Nature Reserve for their field assistance.

References

Alexandris S, Kerkides P. 2003. New empirical formula for hourly estimations of reference evapotranspiration. Agricultural Water Management, 60(3): 157–180.

Anderson D E, Verma S B, Rosenbuerg N J. 1984. Eddy correlation measurements of CO_2, latent heat and sensible heat fluxes over a crop surface. Boundary-Layer Meteorology, 29: 263–272.

Allen R G, Smith M, Pereira L S, et al. 1994. An update for the calculation of reference evaporation. ICID Bulletin, 43(7): 672–674.

Allen R G, Pereira L S, Raes D, et al. 1998. Crop evapotranspiration guidelines for computing crop water requirements-FAO Irrigation and drainage paper 56. FAO, Rome.

Allen R G, Pereira L S, Howell T A, et al. 2011. Evapotranspiration information reporting: I. factors governing measurement accuracy. Agricultural Water Management, 98(6): 899–920.

ASCE-EWRI. 2005. The ASCE standardized reference evapotranspiration equation. In: Allen R G, Walter I A, Elliot R L, et al. Reported by the American Society of Civil Engineers (ASCE) Task Committee on Standardization of Reference Evapotranspiration. ASCE, Reston, 0-7844-0805-X, 204.

Aubinet M, Vesala T, Papale D. 2012. Eddy Covariance: A Practical Guide to Measurement and Data Analysis. Heidelberg: Springer, 365–376.

Burman D, Pochop L O. 1994. Evaporation, evapotranspiration and climatic data. Elsevier Science, 22: 1–5.

Cai J, Liu Y, Lei T, et al. 2007. Estimating reference evapotranspiration with the FAO Penman-Monteith equation using daily weather forecast messages. Agricultural and Forest Meteorology, 145(1–2): 22–35.

De Medeiros G A, Arruda F B, Sakai E. 2005. Crop coefficient for irrigated beans derived using three reference evaporation methods. Agricultural and Forest Meteorology, 135(1–4): 135–143.

Falge E, Baldocchi D, Olson R, et al. 2001. Gap filling strategies for defensible annual sums of net ecosystem exchange. Agricultural and Forest Meteorology, 107(1): 43–69.

Gao Y F, Zhao C Y, Peng S Z, et al. 2015. Evapotranspiration simulation of the grassland and sensitivity analysis in Tianlaochi catchment in the upper reaches of Heihe River. Journal of Desert Research, 35(5): 1338–1345. (in Chinese)

Gu J, Smith E A, Merritt J D. 1999. Testing energy balance closure with GOES-retrieved net radiation and in situ measured eddy correlation fluxes in BOREAS. Journal of Geophysical Research, 104(D22): 27881–27893.

Gu S Y, Tang X, Cui M, et al. 2008. Characterizing evapotranspriration over a meadow ecosystem on the Qinghai-Tibetan plateau. Journal of Geophysical Research, 113: 693–702.

Hou Q, Wang Y S, Yang Z L, et al. 2010. Analysis of control factors of crop coefficient in typical steppe. Chinese Journal of Grassland, 32: 58–64. (in Chinese)

Hou Q, Wang Y S, Shi G H, et al. 2011. Studies on crop coefficients of typical steppe in Inner Mongolia. Acta Prataculturae Sinica, 20(4): 34–41. (in Chinese)

Howell T A, Schneider A D, Jensen M E. 1991. History of lysimeter design and use for evapotranspiration measurements. Lysimeters for evapotranspiration & environmental measurements: Proceedings of the International Symposium on Lysimetry. ASCE, Honolulu, HI, 1–9.

Jensen D, Hargreaves G, Temesgen B, et al. 1997. Computation of ET_0 under nonideal conditions. Journal of Irrigation & Drainage Engineering, 123(5): 394–400.

Jensen M E, Burman R D, Allen R G. 1990. Evapotranspiration and Irrigation Water Requirements. New York: American Society of Civil Engineers, 70–72.

Li J, Wang B, Liu X Q, et al. 2014. A study of fitting an alpine winter pasture evapotranspiration to a model based on the

Penman-Monteith equation. Journal of Animal and Veterinary Advances, 13(3): 123–131.

Li S G, Lai C T, Lee G, et al. 2005. Evapotranspiration from a wet temperate grassland and its sensitivity to microenvironmental variables. Hydrological Processes, 19(2): 517–532.

Lockwood J G. 1999. Is potential evapotranspiration and its relationship with actual evapotranspiration sensitive to elevated atmospheric CO_2 level? Climate Change, 41(2): 193–212.

Mahrt L. 1998. Flux sampling strategy for aircraft and tower observations. Journal of Atmospheric and Oceanic Technology, 15: 416–429.

Massman W J. 2000. A simple method for estimating frequency response corrections for eddy covariance systems. Agricultural and Forest Meteorology, 104(3): 185–198.

Mastrorilli M, Katerji N, Rana G, et al. 1998. Daily actual evapotranspiration measured with TDR technique in Mediterranean conditions. Agricultural and Forest Meteorology, 90(1–2): 81–89.

Mauder M, Foken T. 2004. Documentation and instruction manual of the eddy covariance software package TK2. Work Report University of Bayreuth, Department of Micrometeorology.

Miao H, Chen S, Chen J, et al. 2009. Cultivation and grazing altered evapotranspiration and dynamics in Inner Mongolia steppes. Agricultural and Forest Meteorology, 149(11): 1810–1819.

Mitchell P J, Veneklass E, Lambers H, et al. 2009. Partitioning of evapotranspiration in a semi-arid eucalypt woodland in south-western Australia. Agricultural and Forest Meteorology, 149(1): 25–37.

Molina H P M, Navarro A M, Osorio M C R, et al. 2006. Social and irrigation water management issues in some water user's associations of the Low Segura River Valley (Alicante, Spain). Sustainable Irrigation Management, Technologies and Policies, 96: 205.

Ohmura A. 1982. Objective criteria for rejecting data for Bowen ratio flux calculations. Journal of Applied Meteorology and Climatology, 21(4): 595–598.

Papale D, Reichstein M, Aubinet M, et al. 2006. Towards a standardized processing of net ecosystem exchange measured with eddy covariance technique: algorithms and uncertainty estimation. Biogeosciences, 3: 571–583.

Reichstein M, Falge E, Baldocchi D, et al. 2005. On the separation of net ecosystem exchange into assimilation and ecosystem respiration: review and improved algorithm. Global Change Biology, 11(9): 1424–1439.

Semalty P D, Dev K, Kumar S, et al. 2011. Estimation of forest evapotranspiration over Uttarakhand hills, India. Indian Journal of Physics, 85: 1277–1285.

Simona C, Rita P. 2013. Corrected surface energy balance to measure and model the evapotranspiration of irrigated orange orchards in semi-arid Mediterranean conditions. Irrigation Science, 31(5): 1159–1171.

Song K C, Kang E S, Jin B W, et al. 2004. An experimental study of grassland evapotranspiration in the mountain watershed of the Heihe River Basin. Journal of Glaciology and Geocryology, 26(3): 349–356. (in Chinese)

Stannard D I, Blanford J H, Kustas W P, et al, 1994. Interpretation of surface flux measurements in heterogeneous terrain during the Monsoon '90 experiment. Water Resources Research, 30: 1227–1239.

Sumner D M, Jacobes J M. 2005. Utility of Penman-Monteith, Priestley-Taylor, reference evapotranspiration, and pan evaporation methods to estimate pasture evapotranspiration. Journal of Hydrology, 308(1–4): 81–104.

Sun X M, Zhu Z L, Wen X F, et al. 2006. The impact of averaging period on eddy fluxes observed at ChinaFLUX sites. Agricultural and Forest Meteorology, 137(3–4): 188–193.

Swinbank W C. 1951. The measurement of vertical transfer of heat and water vapour by eddies in the lower atmosphere. Journal of Meteorology, 8(3): 135–145.

Tyagi N K, Sharma D K, Luthra S K. 2000. Determination of evapotranspiration and crop coefficients of rice and sunflower with lysimeter. Agricultural Water Manage, 45(1): 41–54.

Veroustraete F, Verstraeten W W, Feyen J. 2008. Assessment of evapotranspiration and soil moisture content across different scales of observation. Sensors, 8(1): 70–117.

Wever L A, Flanagan L B, Carlson P J. 2002. Seasonal and interannual variation in evapotranspiration, energy balance and surface conductance in a northern temperate grassland. Agricultural and Forest Meteorology, 112(1): 31–49.

Williams L E, Phene C J, Grimes D W, et al. 2003. Water use of mature Thompson seedless grapevines in California. Irrigation Science, 22(1): 11–18.

Williams L E, Ayars J E. 2005. Grapevine water use and the crop coefficient are linear functions of the shaded area measured beneath the canopy. Agricultural and Forest Meteorology, 132(3–4): 201–211.

Wilson K, Goldstein A, Falge E, et al. 2002. Energy balance closure at FLUXNET sites. Agricultural and Forest Meteorology, 113(1–4): 223–243.

Yang F, Zhou G. 2011. Characteristics and modeling of evapotranspiration over a temperate desert steppe in Inner Mongolia,

China. Journal of Hydrological, 396(1–2): 139–147.

Yang Y, Chen R, Han C, et al. 2013. Measurement and estimation of the summertime daily evapotranspiration on alpine meadow in the Qilian Mountains, northwest China. Environmental Earth Sciences, 68(8): 2253–2261.

Zhang F, Zhou G, Wang Y, et al. 2012. Evapotranspiration and crop coefficient for a temperate desert steppe ecosystem using eddy covariance in Inner Mongolia, China. Hydrological Processes, 26(3): 379–386.

Zhao L W, Zhao W Z. 2014. Evapotranspiration of an oasis-desert transition zone in the middle stream of Heihe River, Northwest China. Journal of Arid Land, 6(5): 529–539.

Zhou L, Zhou G. 2009. Measurement and modelling of evapotranspiration over a reed (*Phragmites australis*) marsh in Northeast China. Journal of Hydrology, 372(1–4): 41–47.